Available online at www.sciencedirect.com
SCIENCE DIRECT®
Journal of Catalysis 225 (2004) 381–387
JOURNAL OF CATALYSIS
www.elsevier.com/locate/jcat

Mesostructured aluminosilicate alkylation catalysts for the production of aromatic amine antioxidants

Yu Liu, Seong Su Kim, and Thomas J. Pinnavaia *

Department of Chemistry, Michigan State University, East Lansing, MI 48824-1322, USA

Received 12 January 2004; revised 7 February 2004; accepted 7 April 2004

Available online 25 May 2004

Abstract

The conversion of diphenylamine (DPA) and α-methylstyrene (AMS) to the antioxidants mono- and dicumenyldiphenylamine was carried out over mesostructured aluminosilicate catalysts with hexagonal (2% Al-MCM-41), wormhole (2% Al-HMS), and lamellar/vesicular (2% Al-MSU-G) framework structures. A commercial acid-treated clay catalyst, Engelhard F-20, was included for comparison perposes. The yields of the desired antioxidant, namely dicumenyldiphenylamine (DCDPA), increased in the order F-20 ($\sim$ 57%) < 2% Al-MCM-41 ($\sim$ 85%) < 2% Al-HMS, 2% Al-MSU-G ($\sim$ 90%) when the reaction was carried out under stoichiometric reaction conditions at 90 °C. The DCDPA yields obtained with the mesostructured catalysts are the highest reported to date for this technologically important antioxidant. A heteropolyacid catalyst, $H_3PW_{12}O_{40} \cdot xH_2O$ (PW_{12}) supported on mesostructured wormhole HMS and lamellar/vesicular MSU-G silica, also was examined as a catalyst for DCDPA production. The supported catalyst systems, however, afforded lower maximum yields of DCDPA ($\sim$73–80%) in comparison to the mesostructured aluminosilicate catalysts. The exceptionally high yields of alkylated products obtained with the mesoporous aluminosilicate catalysts in comparison to the F-20 clay and the supported PW_{12} catalysts are attributable in part to intermediate acid strengths that minimize completing dimerization reactions of the AMS alkylating agent. Also, the pore structures of the mesostructured catalysts facilitate access to active sites on the framework walls and provide more efficient transport of reagents to framework reaction centers. Also, the regular mesoporosity of the aluminosilicate catalysts makes these structures less prone to pore plugging and to the masking of acidity through the adsorption of the high molecular weight reaction products.

Keywords: Mesoporous; MCM-41; HMS; MSU-G

1. Introduction

Although zeolite catalysts have been successfully used for the production of fine organic chemicals [1–3] they have limited utility for the transformations of large molecules in the liquid state due to diffusion limitations caused by the restricted pore sizes. Mesostructured aluminosilicates with pores in the 2–50 nm range have been recognized as being potentially superior catalysts over zeolites for condensed phase catalytic reactions, in part, because the large pore size offers the possibility of minimizing diffusion limitations. Indeed, Al-MCM-41 has been shown to be an effective catalyst for the alkylation of a bulky phenol using cinnamyl alcohol as the alkylating agent [4]. Also, a modified form of Al-MCM-41 [5] and a Ga-MCM-41 derivative [6] were shown to be far more active than zeolite Beta for the benzylation of benzene. In addition, $AlCl_3$/MCM-41 [7,8] was found to provide better selectivity toward 2,6-disopropylnaphthalene in the liquid phase isopropylation of naphthalene in comparison to the zeolite mordenite.

Pore size alone, however, is not the only factor favoring the reactivity of mesostructured metal oxide catalysts. The framework pore connectivity and hierarchical structure also are important in facilitating access to the intracrystal active sites of a mesostructure. For example, aluminosilicates with 3D wormhole framework motifs [9,10] are substantially more active than unidimensional MCM-41 for the reduction of NO by NH_3 [11], the cracking of cumene [12,13], and the alkylation [14] and the peroxidation [15] of 2,6-di-*tert*-butylphenol. Similar differences in catalytic activity have been observed between MCM-41 and lamellar mesostruc-

* Corresponding author. Fax: +1-517-432-1225.
E-mail address: pinnavai@cem.msu.edu (T.J. Pinnavaia).

0021-9517/$ – see front matter
doi:10.1016/j.jcat.2004.04.009

tures with a vesicular hierarchical structure that shortens the framework pore length for more facile access to intracrystal active sites [16]. Aside from the significance of framework pore motif in the diffusion of large organic molecules during the condensed-phase alkylation reaction [14], particle size and textural pore between particles are also important. Chmelka and co-workers recently [17] reported that the reaction rate of alkylation of toluene with benzyl alcohol over small particle Al-SBA-15 was much higher than over monolithic particles. As in the case of many other alkylation reactions where diffusion can limit the reaction rates and selectivities [4,18,19] the alkylation of diphenylamine (DPA) is carried out under condensed-phase reaction conditions. Acid-treated and rare earth-modified clays have received considerable attention as catalysts for this industrially important reaction [20–22]. The F-series acid-treated clays provided by Engelhard are especially active catalysts for the alkylation of diphenylamine with α-methylstyrene (AMS) as the alkylating agent [22]. The desired alkylation products are monocumyldiphenylamine (MCDPA) and dicumyldiphenylamine (DCDPA). These products, particularly the dialkylated derivative, are effective antioxidants in many formulations, including hot melt adhesives, polyacetals, nylon 6, polypropylene, polyethylene, ethylene–propylene copolymers and tripolymers, ABS, synthetic lubricants, and polyether polyols, among others. Although 100% conversion of diphenylamine is achieved, the selectivity to DCDPA only reaches 65% with a significant amount of MCDPA and undesired side products being produced. Another drawback was the substantial deactivation of the catalyst after only one batch reaction cycle.

In the present work we have investigated the properties of mesostructured aluminosilicate catalysts for the α-methylstyrene alkylation of diphenylamine. In addition to hexagonal Al-MCM-41 with unidimensional framework pores, we have included in the study Al-HMS and Al-MSU-G mesostructures with wormhole and vesicular (lamellar) framework structures, respectively. As noted above, these latter mesostructures generally provide improved access to framework acid sites in comparison to MCM-41, particularly for large molecules under condensed-phase reaction conditions. It was of interest to us, therefore, to determine whether improved catalytic performance would also be realized for the α-methylstyrene/diphenylamine reaction system. To investigate the effect of acid strength on the yields of DCDPA, we included the strongly acidic Engelhard F-20 clay and several supported versions of the hetero polyacid $H_3PW_{12}O_{40} \cdot xH_2O$ as acid catalysts.

2. Experimental

2.1. Materials

Diphenylamine and α-methylstyrene were obtained form Aldrich and used as purchased. The acid-treated clay F-20 was obtained from Engelhard Corporation (USA). Fumed silica, tetraethylorthosilicate (TEOS), dodecylamine (DDA), cetyltrimethylammonium bromide (CTAB), tetramethylammonium hydroxide (TMAOH), the 12-tungstophosphoric acid $H_3PW_{12}O_{40} \cdot xH_2O$ (PW_{12}) and 2,6-di-*tert*-butylpyridine were purchased from Aldrich.

2.2. 2% Al-MCM-41

A mixture of fumed silica, cetyltrimethylammonium bromide, trimethylammonium hydroxide, and water was stirred at room temperature for 1 h and then transferred into an autoclave. The synthesis gel was heated at 150 °C for 24 h in an autoclave to obtain a hexagonal MCM-41 silica. The autoclave was cooled to room temperature and an amount of $Al(NO_3)_3$ sufficient to provide a Si/Al molar ratio of 49 was added under stirring. The resulting mixture of molar composition $1.00SiO_2$:$0.02Al(NO_3)_3$:0.20CTAMBr:0.26TMAOH:$110H_2O$ was further heated at 150 °C for another 24 h. The final product was filtered, washed, dried at room temperature, and calcined in air at 600 °C for 4 h to remove the surfactant.

2.3. 2% Al-HMS

Tetraethylorthosilicate was added to a mixture of dodecylamine (DDA), water, ethanol (EtOH), and mesitylene (MES) at room temperature. The mixture was stirred for 1 h and then $Al(OBu^s)_3$ in *sec*-butanol was added under stirring. After a reaction time of 24 h at room temperature, the solid was filtered, washed, dried at room temperature, and caclined in air at 620 °C for 4 h. The molar ratio of the above synthesis mixture was $1.00SiO_2$:0.02Al:0.25DDA:1.12MES:5.0ETOH:$130H_2O$.

2.4. 2% Al-MSU-G

The pure silica form of MSU-G was prepared by reaction of TEOS, neutral Gemini surfactant $C_{12}H_{25}NH(CH_2)_2NH_2$, EtOH, and water under hydrothermal conditions according to our previously reported procedure [16,23]. $Al(OBu^s)_3$ was added to the as-synthesized silica MSU-G in its mother liquor to achieve an overall Si/Al ratio of 49:1. The resultant mixture was heated again at 100 °C for 48 h under stirring. The final solid was filtered, washed with water and ethanol, air dried, and calcined at 650 °C for 4 h.

2.5. Supported $H_3PW_{12}O_{40}$(PW_{12}) catalysts

Calcined forms of mesostructured HMS and MSU-G silicas were prepared according to the procedures described above without the addition of $Al(OBu^s)_3$ to the reaction mixture. The pure silica mesostructures were dried at 150 °C under vacuum conditions for 5–10 h and impregnated with a methanol solution containing the desired amount of $H_3PW_{12}O_{40}$. The mixture was stirred at room temperature

for 24 h and then the methanol was removed under vacuum at room temperature. The impregnated solid was then dried at 130 °C under vacuum for 10 h.

2.6. Physical measurements

Powder X-ray diffraction patterns were measured using Cu-Kα radiation ($\lambda = 1.542$ Å) and a Rigaku Rotaflex diffractometer equipped with a rotating anode operated at 45 kV and 100 mA. Counts were accumulated every 0.02° (2θ) at a scan speed of 1°2θ min^{-1}. N_2 adsorption and desorption isotherms were obtained at −196 °C on a Micromeritics ASAP 2010 sorptometer using static adsorption procedures. Samples were outgassed at 150 °C and 10^{-6} Torr for a minimum 12 h prior to analysis. BET surface areas were calculated from a linear part of the BET plot according to IUPAC recommendations. Pore-size distributions were calculated from the N_2 adsorption branch using the Horvath–Kawazoe model.

TEM images were obtained on a JEOL 100CX microscope equipped with a CeB_6 gun operated at an acceleration voltage of 120 kV. The specimen was loaded onto a holey carbon film that was supported on a copper grid by dipping the grid into a sample suspension in ethanol.

The acidities of 2% Al-HMS, 2% Al-MCM-41, and F-20 were measured by means of thermogravimetric analysis (TGA) analysis of chemisorbed 2,6-di-*tert*-butylpyridine in the temperature range of 150–600 °C [24]. The samples were exposed to liquid 2,6-di-*tert*-butylpyridine at 80 °C for 4 h and then kept at room temperature overnight so as to allow the base to permeate the samples. TGA curves were obtained using a CAHN121 TGA analyzer. The samples were purged with N_2 at 150 °C for 1 h to removal the physically adsorbed 2,6-di-*tert*-butylpyridine then heated to 600 °C at a heating rate of 10 min/°C. The molecule sizes of MCDPA and DCDAP were calculated by Spartan software. The amount of organic compounds trapped in the used catalysts was measured by TGA in the temperature range of 150–800 °C in an air flow. Prior to the TGA measurement, the used catalysts were washed thoroughly with methanol.

2.7. Catalytic studies

The catalytic reactions were performed in a 25-ml three-necked flask containing the desired amount of diphenylamine and α-methylstyrene. The reactions were carried out at 90 °C for 6–24 h. Prior to reaction, the catalysts were dried under vacuum at 100 °C for 8 h. The reaction products were analyzed by GC on a HP 5890 instrument equipped with a FID detector. A 15-m SPB-1 capillary column was used for the analysis of diphenylamine, α-methylstyrene, and mono- and dicumyldiphenylamine. The monocumyldiphenylamine and dicumyldiphenylamine were separated from the reaction mixtures by fractional distillation and their structures were verified by GC-MS, ^{1}H NMR, and ^{13}C NMR. The properties of the isolated products were identical to those of authentic MCDPA and DCDPA samples.

3. Results and discussion

3.1. Structural and textural properties of the catalysts

Fig. 1 provides the low angle X-ray powder diffraction patterns for 2% Al-MCM-41, 2% Al-HMS, and 2% Al-MSU-G aluminosilicate mesostructures with hexagonal, wormhole and lamellar/vesicular framework morphologies, respectively. Included for comparison purposes are the patterns for the supported PW_{12}-HMS and PW_{12}-MSU-G catalysts, wherein the wormhole HMS and lamellar/vesicular MSU-G silicas, respectively, have been intercalated at the 20 wt% level with the heteropoly acid $H_3PW_{12}O_{40}$. The 2% Al-MCM-41 mesophase exhibits four *hkl* diffraction lines consistent with the expected hexagonal framework structure. However, the wormhole and lamellar frameworks of HMS and MSU-G, as well as the corresponding derivatives intercalated by the heteropoly acid $H_3PW_{12}O_{40}$, each exhibit a single diffraction line. TEM images, shown in Fig. 2, verify the wormhole and lamellar/vesicular structure assignments for the HMS and MSU-G mesophases, as well as the hexagonal framework structure for MCM-41.

The textural properties of the aluminosilicate mesophases, together with those for the commercial acid-treated F-20 clay and PW_{12}-intercalated HMS catalysts, are provided in Table 1. The surface areas, as determined by fitting the BET equation to nitrogen adsorption isotherms in the partial pressure region below a partial pressure of 0.30, decreased in the order 2% Al-MCM-41 > 2% Al-HMS > 2% Al-MSU-G >

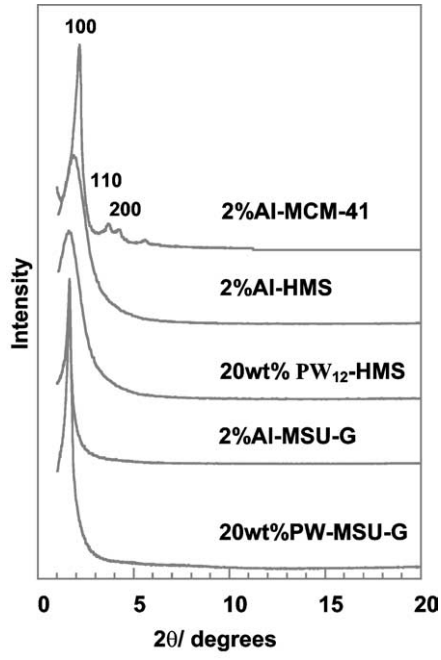

Fig. 1. Low angle XRD patterns of alkylation catalysts.

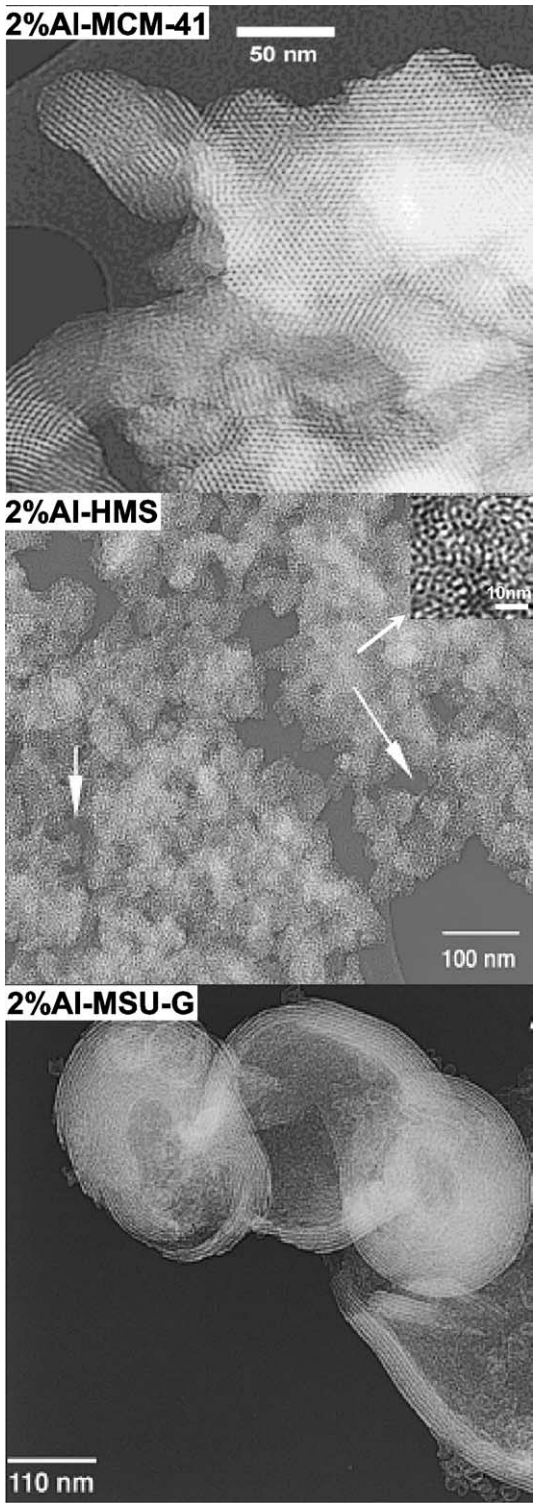

Fig. 2. TEM images showing the hexagonal framework pore structure of 2% Al-MCM-41, the intraparticle textural pores (arrows) and the wormhole framework structure (insert) of 2% Al-HMS, and the lamellar/vesicular structure of 2% Al-MSU-G.

F-20. As will be shown below, the activities and selectivities of these catalysts for diphenylamine alkylation did not parallel the BET surface areas. Note that the mesostructured catalysts have framework pore sizes are in the range 3.4–3.8 nm,

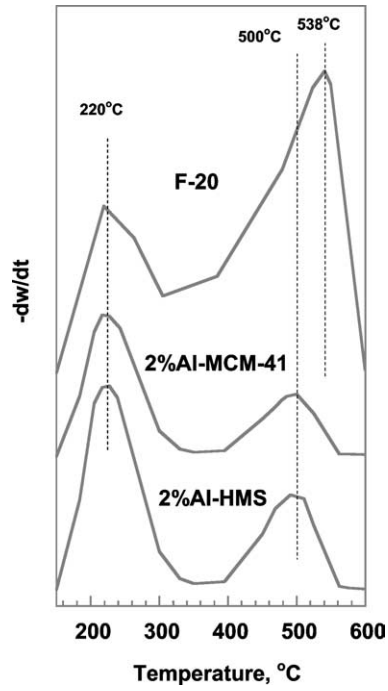

Fig. 3. Thermally programmed desorption of 2,6-di-*tert*-butylpyridine over F-20 clay and mesostructured 2% Al-MCM-41 and 2% Al-HMS aluminosilicate catalysts.

sufficiently large to accommodate both the DPA starting reagent and the DCDPA reaction product with molecular dimensions of $0.91 \times 0.49 \times 0.52$ and $1.66 \times 0.66 \times 0.72$ nm, respectively, as estimated using SPARTAN software. The acid-treated F-20 clay catalyst lacks framework mesoporosity. Intercalating mesostructured wormhole framework of HMS silica with up to 20 wt% $H_3PW_{12}O_{40}$ did not substantially affect the pore size or the surface area of the host structure.

In order to judge the relative acidity of the mesostructured catalysts in comparison to the acid-treated F-20 clay catalyst, we examined the temperature-programmed desorption of chemisorbed 2,6-di-*tert*-butylpyridine from each catalyst. The desorption curves for F-20 clay, 2% Al-MCM-41, and 2% Al-HMS mesostructures are shown in Fig. 3. The total amount of chemisorbed 2,6-di-*tert*-butylpyridine was somewhat greater for the F-20 clay (0.21 mmol/g) than for the mesostructures (0.13–0.17 mmol/g). Although each catalyst showed bimodal acid strengths, as reflected by the presence of low and high temperature desorption peaks, the high temperature desorption peak occurred at 538 °C for the clay catalyst, whereas the corresponding peak for the mesostructured catalyst was centered near 500 °C. Thus, the clay catalyst exhibited not only more acid sites in comparison to the mesostructured catalysts, but also stronger acid sites. Also, access to the acid sites of each catalyst by the 2,6-di-*tert*-butylpyridine molecule, with the approximate molecular dimensions of $0.75 \times 0.69 \times 0.43$ nm, was not limited by pore-size considerations.

Table 1
Textural properties of alkylation catalysts[a]

Catalyst	Framework structure	BET surface; area (m^2/g)	Pore vol. (cc/g)[b]	HK pore size (nm)	Acidity (mmol DBPD/g)
2% Al-MCM-41	Hexagonal	907	1.0	3.6	0.13
2% Al-HMS	Wormhole	812	1.3	3.8	0.17
10% PW_{12}-HMS	Wormhole	890	1.5	4.3	–
20% PW_{12}-HMS	Wormhole	876	1.3	4.2	–
2% Al-MSU-G	Lamellar/vesicular	444	0.57	3.4	–
F-20 clay	None	380	0.38	–	0.21

[a] Samples were out-gassed at 150 °C for 24 h prior to the determination of textural properties by nitrogen adsorption.
[b] The reported pore volumes were obtained from the nitrogen uptake at $P/P_0 = 0.98$.

3.2. Catalytic properties of mesostructured aluminosilicates

The alkylation of diphenylamine to monocumyldiphenylamone and dicumyldiphenylamine with α-methylstyrene as the alkylating reagent is represented in Scheme 1.

As is shown by the catalytic results presented in Table 2 for the reaction at a stoichiometric DPA:AMS molar ratio of 1:2, all three mesostructured aluminosilicates provide more than 90% conversion of DPA after a reaction time of 6 h at 90 °C. An even higher DPA conversion (∼ 99%) is achieved with the acidic F-20 clay under equivalent reaction conditions. However, the mesostructured catalysts afford primarily the mono- and dialkylated products at this point in the reaction, whereas the F-20 clay catalyst provides substantial fractions of other reaction products. These latter features of the catalysts can be gleaned from the product distributions obtained by extending the reaction time to 24 h. All four catalysts provide 100% conversions of DPA after 24 h, but only the mesostructured catalysts transformed monoalkylated amine to dialkylated amine under these reaction conditions, resulting in DCDPA yields of ∼ 90%. However, the DCDPA yield obtained with the F-20 clay catalyst is only marginally improved from 52.8 to 56.7% by extending the reaction time from 6 to 24 h, indicating that competing reactions deplete the AMS alkylating agent and limit the yield of the desired dialkylated antioxidant. The unsaturated AMS alkylating agent is known to form dimeric species in the presence of strong acid catalysts [25] according to the reaction Scheme 2.

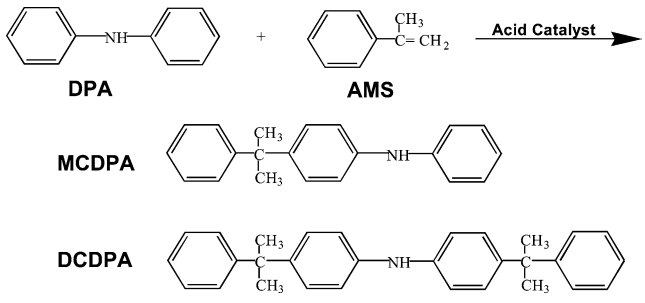

Scheme 1. The scheme of alkylation of DPA with AMS.

We attribute analogous dimerization reactions to the depletion of the AMS alkylating agent with F-20 clay as the alkylation catalyst. This acid-washed quasicrystalline aluminosilicate is known to be sufficient in acid strength to promote dimerization of AMS [26]. Moreover, the acidity of F-20 clay has been reported to be even stronger than sulfated zirconia and proton-exchanged resins for the alkylation of 4-methoxyphenol with MTBE [27]. On the other hand, mesostructured aluminosilicates with amorphous framework walls are recognized as being considerably weaker acid catalysts [28,29]. Independent verification of the relative acid strengths of F-20 clay in comparison to 2% Al-HMS and 2% Al-MSU-G is provided by the thermogravimetric desorption curves for 2,6-di-*tert*-butylpyridine in Fig. 3. The peak desorption rate occurs at a substantially higher temperature for the clay catalyst (538 °C) in comparison to the mesostructured catalysts (500 °C). Thus, the lower acidity for the mesostructures suggests that they should be less prone to form high surface concentrations of onium ions through alkyl group protonation and, therefore, less likely to promote AMS dimerization reactions.

Because the yields of the desired dialkylated antioxidant are limited by the consumption of the alkylating agent through the dimerization reactions shown in Scheme 2, we repeated the alkylation reaction at a DPA:AMS ratio of 1:3 (see Table 2). As expected in the presence of excess alkylating agent, the conversion of DPA was complete after a reaction time of 6 h, and the yields of DCDPA increased at the expense of MCDPA in comparison to the reactions carried out at a 1:2 DPA:AMS molar ratio.

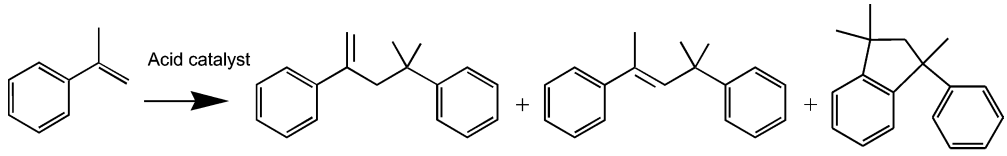

Scheme 2.

Table 2
Aluminosilicate catalysts for the conversion of diphenylamine (DPA) at 90 °C to monocumyldiphenylamine (MCDPA) and dicumyldiphenylamine (DCDPA) with α-methylstyrene (AMS) as the alkylating agent[a]

Catalyst	Rxn time (h)	DAP:AMS ratio	DPA conv. (%)	Distribution of alkylated products (%)		Yield of DCDPA (%)
				MCDPA	DCDPA	
2% Al-MCM-41	6.0	1:2	93.7	27.5	72.5	67.9
	24.0	1:2	100	14.9	85.1	85.1
2% Al-HMS	6.0	1:2	95.8	25.6	74.4	71.3
	24.0	1:2	100	8.9	90.1	90.1
2% Al-MSU-G	6.0	1:2	96.7	23.8	76.2	73.7
	24.0	1:2	100	8.7	91.3	91.3
F-20	6.0	1:2	98.7	46.5	53.5	52.8
F-20	24.0	1:2	100	43.3	56.7	56.7
2% Al-MCM-41	6.0	1:3	100	20.5	79.5	79.5
2% Al-HMS	6.0	1:3	100	3.5	96.5	96.5
2% Al-MSU-G	6.0	1:3	100	2.8	97.2	97.2
F-20	6.0	1:3	100	35.2	64.5	64.5

[a] The amount of catalyst used was 1.0 g per 0.050 mol AMS (DPA:AMS = 1:2) or 0.075 mol AMS (DPA:AMS = 1:3).

Table 3
Mesostructure-supported phosphotungstic acid (PW_{12}) for the catalytic conversions of diphenylamine (DPA) at 90 °C to monocumyldiphenylamine (MCDPA) and dicumyldiphenylamine (DCDPA) with α-methylstyrene (AMS) as the alkylating agent[a]

Catalyst	Rxn time (h)	DAP:AMS ratio	DPA conv. (%)	AMS conv. (%)	Distribution of alkylated products (%)		Yield of DCDPA (%)
					MCDPA	DCDPA	
10% PW_{12}-HMS	6.0	1:2	93.5	100	22.1	77.9	72.8
20% PW_{12}-HMS	6.0	1:2	93.8	100	18.9	81.1	76.0
10% PW_{12}-MSU-G	6.0	1:2	94.2	100	18.4	81.6	76.9
20% PW_{12}-MSU-G	6.0	1:2	96.5	100	17.6	82.4	79.5

[a] The amount of catalyst used was 1.0 g per 0.050 mol AMS.

In order to investigate the longevity of the mesostructured aluminosilicate catalysts for the conversion of DPA to DCDPA under stoichiometric reaction conditions, the catalysts were recovered after the first reaction cycle, washed with ethanol, and subjected to a second 24-h reaction cycle at 90 °C. Within experimental uncertainty, the mesostructured catalysts afforded the same DPA conversions (100%) and high yields ($\geqslant$ 85%) of dialkylated antioxidant that was achieved in the first cycle. However, the DPA conversion and the PCDPA product yield obtained with the F-20 clay catalyst dropped from 100 and $\sim$ 57%, respectively, in the first cycle, to 74 and 31% in the second cycle. The loss of alkylation reactivity for analogous acid-washed clay catalysts has been noted previously and attributed to micropore blocking and the loss of acid sites by adsorbed reaction products [22]. These adsorbed components led to a decrease in the surface area and to the masking of acid sites on the surface of the catalyst. Indeed, we find that the F-20 clay looses $\sim$ 23% of its normalized nitrogen BET surface area after the first reaction cycle due to the adsorption of 20% by weight of the high molecular weight reaction products in the micropores. However, the normalized surface areas and the mesopore sizes of the mesostructured aluminosilicate catalysts remained unchanged after the first reaction cycle.

3.3. Catalytic properties of mesostructure-supported $H_3PW_{12}O_{40}$

Mesostructured silicas have been shown to be effective supports for the immobilization of the heteropoly acid $H_3PW_{12}O_{40}$ (PW_{12}) for acid-catalyzed phenol alkylations [30,31] and *iso*-butane/butene alkylation [32]. Similar activity may be anticipated for the alkylation of DPA. Accordingly, we have examined the conversion of DPA and AMS over $H_3PW_{12}O_{40}$ supported on wormhole HMS and lamellar/vesicular MSU-G silicas.

Table 3 provides the yields of the desired DCDPA antioxidant obtained at $H_3PW_{12}O_{40}$ loadings of 10 and 20% (w/w), a DPA:AMS molar ratio of 1:2 and a reaction time of 6 h at 90 °C. Under these reaction conditions the AMS alkylating reagent is completely depleted from the reaction mixture owing to its reaction with DPA to form mono- and dialkylated reaction products and, notably, to the competitive dimerization reaction according to reaction (Scheme 2) above. Due to the depletion of AMS through dimerization, the yields of the desired DCDPA antioxidant are maximized after a reaction time of 6.0 h or less to values of 73–76 and 77–80% for PW_{12} supported on HMS and MSU-G silicas, respectively. As expected, increasing the reaction time over these catalysts to 24 h resulted in no improvement in DCDPA yields.

Although the rates of alkylation are slower over 2% Al-HMS and 2% Al-MSU-G, resulting in DCDPA yields of 71.3 and 73.7% after 6.0 h reaction times, the AMS dimerization rates for these catalysts also are lower. Thus, increasing the reaction time over these latter catalysts to 24 h boosts the yields of DCDPA to values of 90.1 and 91.3% (cf. Table 2). Thus, the mesostructure-supported $H_3PW_{12}O_{40}$ catalysts are substantially less selective alkylation catalysts than the corresponding aluminated mesostructures. It appears that the high acid strength of the supported $H_3PW_{12}O_{40}$ catalysts, which compromises the alkylation of both DPA and MCDPA through AMS dimerization, causes the catalytic properties to be similar to those of the strong acid F-20 clay catalyst.

4. Conclusions

All of the solid acid catalyst examined in this study are effective in converting diphenylamine to monocumyldiphenylamine in an initial alkylation step using α-methylstyrene as the alkylating agent (cf. Tables 2 and 3). However, the hexagonal 2% Al-MCM-41, wormhole 2% Al-HMS, and lamellar/vesicular 2% Al-MSU-G mesostructures are substantially more selective in comparison to the commercial F-20 clay and supported $H_3PW_{12}O_{40}$ catalysts for the conversion of MCDPA to the desired dicumyldiphenylamine antioxidant in a second alkylation step.

The superior selectivity of the aluminosilicate mesostructures for the second alkylation process is attributable in part to an acid strength that allows for the protonation of the α-methylstyrene and coadsorption of MCDPA, while at the same time minimizing the surface concentration of α-methylstyrene for conversion to undesired dimers. At an initial DPA:AMS reaction stoichiometry of 1:2, $\sim$ 27% of the AMS alkylating agent is converted to dimeric products over the commercial F-20 clay catalyst, and $\sim$ 12–15% of the alkylating agent is lost to dimeric products over the mesostructure-supported $H_3PW_{12}O_{40}$ catalysts. Thus, these competing dimerization reactions limit the DCDPA yields to only 57% for the F-20 clay and to 73–80% in the case of the supported $H_3PW_{12}O_{40}$ catalysts, depending on the 12-tungstophosphoric acid loading and the framework structure of the support. In comparison, the hexagonal, wormhole and lamellar/vesicular aluminosilicate mesostructures convert only 7.5, 5.0, and 4.4% of AMS to dimeric products, respectively, under the same reaction conditions. By minimizing the competing dimerization reaction of the alkylating agent, the hexagonal, wormhole and lamellar/vesicular aluminosilicate mesostructures provide DCDPA yields of 85, 90, and 91%, respectively. These latter values represent the highest yields reported to date for this technologically important antioxidant under stoichiometric reaction conditions.

Finally, the regularly mesoporous aluminosilicates silicate catalysts show good longevity and recyclability in comparison to the commercial F-20 clay catalyst by being less prone to the masking of acidity through the adsorption of reaction products.

Acknowledgment

The support of this research by the National Science Foundation through CRG Grant CHE-0211029 is gratefully acknowledged.

References

[1] A. Corma, Chem. Rev. 95 (1995) 559.
[2] A. Corma, Chem. Rev. 97 (1997) 2373.
[3] A. Corma, H. Garcia, Catal. Today 38 (1997) 257.
[4] E. Armengol, M.L. Cano, A. Corma, H. Garcia, M.T. Navarro, Chem. Commun. (1995) 519.
[5] S. Jun, S.H. Joo, R. Ryoo, M. Kruk, M. Jaroniec, Z. Liu, T. Ohsuna, O. Terasaki, J. Am. Chem. Soc. 122 (2000) 10712.
[6] K. Okumura, K. Nishigaki, M. Niwa, Micropor. Mesopor. Mater. 44–45 (2001) 5096.
[7] X.S. Zhao, G.Q. Lu, C. Song, Chem. Commun. (2001) 2306.
[8] X.S. Zhao, G.Q. Lu, C. Song, J. Mol. Catal. A: Chem. 191 (2003) 67.
[9] P.T. Tanev, T.J. Pinnavaia, Science 267 (1995) 865.
[10] S.A. Bagshaw, E. Prouzet, T.J. Pinnavaia, Science 269 (1995) 1242.
[11] W. Zhang, T.R. Pauly, T.J. Pinnavaia, Chem. Mater. 9 (1997) 2491.
[12] K.R. Kloetstra, J.C. Jansen, Chem. Commun. (1997) 2281.
[13] R. Mokaya, W. Jones, J. Catal. 172 (1997) 211.
[14] T.R. Pauly, Y. Liu, T.J. Pinnavaia, S.J.L. Billinge, T.P. Rieker, J. Am. Chem. Soc. 121 (1999) 8835.
[15] P.T. Tanev, M. Chibwe, T.J. Pinnavaia, Nature 368 (1994) 321.
[16] S.S. Kim, Y. Liu, T.J. Pinnavaia, Micropor. Mesopor. Mater. 44 (2001) 489.
[17] J.J. Chiu, D.J. Pine, S.T. Bishop, B.F. Chmelka, J. Catal. 221 (2004) 400.
[18] E.G. Derouane, C.J. Dillon, D. Bethell, S.B. Derouane-Abd Hamid, J. Catal. 187 (1999) 209.
[19] E.G. Derouane, G. Crehan, C.J. Dillon, D. Bethell, H. He, S.B. Derouane-Abd Hamid, J. Catal. 194 (2000) 410.
[20] J.T. Lai, D.S. Filla, EP 810 200, 1997.
[21] J.T. Lai, D.S. Filla, U.S. 5 672 752, 1998.
[22] S.R. Chitnis, M.M. Sharma, J. Catal. 160 (1996) 84.
[23] S.S. Kim, W.Z. Zhang, T.J. Pinnavaia, Science 282 (1998) 1302.
[24] A. Corma, V. Fornes, L. Forni, F. Marquez, J. Martinez-Triguero, D. Moscotti, J. Catal. 179 (1998) 451.
[25] A. Heidekum, M. Harmer, W.F. Holderich, Catal. Lett. 47 (1997) 243.
[26] B. Chaudhuri, M.M. Sharma, Ind. Eng., Chem. Res. 28 (1989) 1757.
[27] G.D. Yadav, M.S.M. Mujeebur Rahuman, Appl. Catal. A 253 (2003) 113.
[28] A. Corma, V. Fornes, M.T. Navarro, J. Perez-Pariente, J. Catal. 148 (1994) 569.
[29] A. Corma, M.S. Grande, V. Gonzalez-Alfaro, A.V. Orchilles, J. Catal. 159 (1996) 375.
[30] I.V. Kozhevnikov, K.R. Kloetstra, A. Sinnema, H.W. Zandbergen, H. van Bekkum, J. Mol. Catal. A: Chem. 114 (1996) 287.
[31] I.V. Kozhevnikov, A. Sinnema, R.J.J. Jansen, K. Pamin, H. van Bekkum, Catal. Lett. 30 (1995) 241.
[32] W. Chu, Z. Zhao, W. Sun, X. Ye, Y. Wu, Catal. Lett. 55 (1998) 57.